lncRNA HOTAIR mediates OGD/R-induced cell injury and angiogenesis in a EZH2-dependent manner

YUNPENG WANG[1], JIAOYU MAO[1], XIAODONG LI[1], BEIBEI WANG[2] and XIAOGUANG ZHOU[2]

[1]Department of Neonatology, Huazhong University of Science and Technology Union Shenzhen Hospital, Shenzhen, Guangdong 518052; [2]Department of Neonatology, Children's Hospital of Nanjing Medical University, Nanjing, Jiangsu 210008, P.R. China

Received April 21, 2021; Accepted July 22, 2021

DOI: 10.3892/etm.2021.11022

Abstract. Long non-coding RNAs (lncRNA) serve an important role in neonatal hypoxic-ischemic encephalopathy (HIE) have been reported to regulate the activity of HIE-associated proteins. The present study aimed to elucidate the role of Hox transcript antisense intergenic RNA (HOTAIR) in oxygen-glucose deprivation/reperfusion (OGD/R)-induced injury in human brain microvascular endothelial cells (hBMVECs). The levels of HOTAIR were evaluated in the serum of neonatal patients with HIE, and the effects of HOTAIR were evaluated using *in vitro* assays, such as reverse transcription-quantitative PCR to detect lncRNA and mRNA levels and western blot analysis to determine protein levels. Moreover, RNA immunoprecipitation assays were used to evaluate the association between HOTAIR and enhancer of zeste homolog 2 (EZH2), Cell Counting Kit-8 was used to detect cell viability, an endothelial monolayer cell permeability assay was used to analyze cell viability, TUNEL staining was used to detect the levels of apoptosis, a Transwell assay was used to evaluate cell invasion and a tube formation assay was used to analyze tube formation ability. In addition, the effects of HOTAIR and EZH2 on cell apoptosis and the invasive and tube formation abilities of hBMVECs were investigated using TUNEL, Transwell and tube formation assays, respectively. The results showed that the expression levels of HOTAIR were markedly increased both in neonatal HIE patients and in the OGD/R injury *in vitro* model. HOTAIR knockdown reduced hBMVEC viability, enhanced cell permeability and apoptosis, in addition to decreasing the expression levels of tight junction-related proteins, such as zonula occludens-1, occluden, Claudin5 and vascular endothelial-cadherin. However, EZH2 overexpression reversed the effects of HOTAIR silencing on hBMVECs. Additionally, HOTAIR knockdown enhanced the migratory and tube formation abilities of OGD/R-induced hBMVECs, which were also reversed by EZH2 overexpression. Overall, the present study revealed an association between the HOTAIR/EZH2 axis and brain microvascular endothelial cell injury and angiogenesis, which provides a novel insight into the molecular mechanism underlying stroke or the development of new pharmacotherapies.

Introduction

Neonatal hypoxic-ischemic encephalopathy (HIE) is a common complication of neonatal asphyxia that may lead to cerebral hypoxic-ischemic damage, cerebral palsy, intellectual retardation and epilepsy and is a leading cause of neonatal mortality and disability (1-3). The pathogenesis of HIE is complex and has been proposed to be associated with abnormal hemorheology (4). Compromised integrity of the blood-brain barrier (BBB) caused by ischemia/reperfusion (IR) injury may lead to secondary brain damage after infarction, with symptoms including brain edema and hemorrhage (5). Preserving the integrity of the BBB is considered to be one of the most important therapeutic strategies for alleviating cerebral infarction injury (6). Cerebrovascular endothelial cells normally create the BBB between brain and the rest of the circulation and exhibit a variety of secretory functions (7). Therefore, microvascular endothelial cell injury is closely associated with the occurrence and development of cerebrovascular diseases (8,9).

A previous study revealed a significant difference either in the upregulation or downregulation of the expression levels of 255 long non-coding RNAs (lncRNAs) in serum samples isolated from rats that underwent middle cerebral artery occlusion, compared with a sham group (10). Hox transcript antisense intergenic RNA (HOTAIR) is an important lncRNA that is encoded by the antisense chain of the HOXC11 gene in the 2q13.13 chromosomal region and transcribed by RNA polymerase (11). Emerging evidence has suggested that lncRNAs can serve important roles in a number of diseases, including atherosclerosis, stroke and aneurysm (12,13). A previous study demonstrated that the expression level of lncRNA HOTAIR was upregulated in neurons following

Correspondence to: Dr Xiaoguang Zhou, Department of Neonatology, Children's Hospital of Nanjing Medical University, 72 Guangzhou Road, Nanjing, Jiangsu 210008, P.R. China
E-mail: zhouxxiaoguang@163.com

Key words: lncRNA HOX transcript antisense intergenic RNA, enhancer of zeste 2 polycomb repressive complex 2 subunit, oxygen-glucose deprivation/reperfusion, tight junctions

cerebral IR injury, compared with healthy neurons (1). In addition, lncRNA HOTAIR downregulation was found to promote burn-induced angiogenesis in umbilical vein endothelial cells (14). However, to the best of our knowledge, the role of HOTAIR in oxygen-glucose deprivation/reperfusion (OGD/R)-induced brain endothelial cell injury has not been previously studied.

Enhancer of zeste homolog 2 (EZH2) is a histone methyltransferase that has been documented to be involved in IR injury (15). Previous studies have demonstrated that EZH2 knockdown conferred a neuroprotective role in ischemic brain injury (16-18). Another study revealed that EZH2 inhibition can regulate microglial activation and inflammation following hypoxic-ischemic brain injury, where it could promote autophagy through the PTEN/AKT/mTOR signaling pathway (19). Furthermore, following IR injury, the expression level of EZH2 was found to be upregulated in microglia, compared with a sham group (16). It has also been proposed that the protein stability of EZH2 is regulated by several lncRNAs including lncRNA ANCR and lncRNA FAM83C-AS1 (20). Previous studies demonstrated that the interaction between EZH2 and different lncRNAs, such as lncRNA ANCR and lncRNA HERES can suppress cancer cell invasion, including breast cancer and esophageal squamous cell carcinoma (21,22).

Therefore, the present study aimed to investigate the role of HOTAIR in neonatal HIE and its association with EZH2 in OGD/R-induced human brain microvascular endothelial cells (hBMVECs).

Materials and methods

Clinical data. In the present study children who met the diagnostic criteria of neonatal HIE as described previously (23) were enrolled between January 2020 and January 2021, including 2 males and 3 females (age, <24 h), with a gestational age of 38-42 weeks and a birth weight of 2.6-3.9 kg. All children had a history of asphyxia, caused by umbilical cord prolapse and compression and around the neck. All children were delivered in the Huazhong University of Science and Technology Union Shenzhen Hospital (Shenzhen, China).

In addition, five normal-term newborns, including two males and three females, who were delivered in the Huazhong University of Science and Technology Union Shenzhen Hospital (Shenzhen, China) during the same time period, were also enrolled. In the five HIE cases aforementioned, the respective mothers did not experience intrauterine infections or intrauterine or postpartum asphyxia, and did not receive immune agents or blood products, including various human plasma protein products during gestation.

A total of 3 ml venous blood was collected from neonates in both groups after birth. Following centrifugation at 400 x g for 40 min at 25˚C, the serum was collected and stored in a -70˚C refrigerator for subsequent experiments. The present study was approved by the Ethics Committee of Huazhong University of Science and Technology Union Shenzhen Hospital. Written informed consent for blood collection was obtained from the legal guardians of each child.

Cell culture. Human brain microvascular endothelial cells (hBMVECs; cat. no. CP-H124; Procell Life Science & Technology Co., Ltd.) were cultured in Procell Life Science & Technology Co., Ltd. medium supplemented with 10% FBS and 100 μl/ml penicillin/streptomycin (all Procell Life Science & Technology Co., Ltd.) at 37˚C in a water-saturated atmosphere of 5% CO_2 and 95% air. The cells were dispersed with 0.25% trypsin and were then sub-cultured. Cells in the logarithmic growth phase were selected for subsequent experiments.

Establishment of OGD/R injury in vitro model. hBMVECs were first seeded into 35-mm diameter dishes at a density of $1x10^6$ cells/well. After 24 h at 37˚C, the cells adhered to the dish walls. Following washing with sugar-free Earle's balanced salt solution (sugar-free OGD solution; Thermo Fisher Scientific, Inc.), the medium was replaced with glucose-free, serum-free culture medium at 37˚C. The cells were then cultured in a modified closed OGD tank at an atmosphere of 1% O_2, 5% CO_2 and balanced N_2 for 2 h at 37˚C before being incubated in Procell Life Science & Technology Co., Ltd. medium in a humidified incubator at 37˚C for re-oxygenation for 12, 24 or 48 h. The cells in the control were cultured in serum-free medium at 37˚C with 5% CO_2.

Reverse transcription-quantitative PCR (RT-qPCR). RT-qPCR assay was performed to measure the expression levels of the target genes in each group after RNA extraction using TRIzol® reagent (Thermo Fisher Scientific, Inc.) for 10 min, followed by centrifugation at 4˚C and 13,514 x g (centrifugation radius, 10 cm) for 15 min. Subsequently, the cell-TRIzol® mixture was transferred into 1.5-ml microcentrifuge tubes without RNase. The reverse transcription process was performed with a First Strand cDNA Synthesis Kit (cat. no. K1073; APExBIO Technology LLC) and then qPCR was performed using a qPCR kit (Sigma-Aldrich; Merck KGaA). Thermocycling conditions were as following: Initial denaturation at 95˚C for 3 min, followed by 39 cycles of 95˚C for 30 sec, 55˚C for 20 sec and 72˚C for 20 sec. GAPDH served as the internal reference gene and results were analyzed using the $2^{-\Delta\Delta Cq}$ method (24). The primers sequences used in this study are as follows: HOTAIR forward, 5'-ATAGGCAAATGTCAGAGGGTT-3' and reverse, 5'-ATTCTTAAATTGGGCTGGGTC-3'; EZH2 forward, 5'-AATCAGAGTACATGCGACTGAGA-3' and reverse, 5'-GCTGTATCCTTCGCTGTTTCC-3'; zonula occludens-1 (ZO-1) forward, 5'-CAACATACAGTGACG CTTCACA-3' and reverse, 5'-CACTATTGACGTTTCCCC ACTC-3'; occludin forward, 5'-ACAAGCGGTTTTATC CAGAGTC-3' and reverse, 5'-GTCATCCACAGGCGAAGT TAAT-3'; Claudin-5 forward, 5'-CTCTGCTGGTTCGCC AACAT-3' and reverse, 5'-CAGCTCGTACTTCTGCGA CA-3'; vascular endothelial (VE)-cadherin forward, 5'-TTG GAACCAGATGCACATTGAT-3' and reverse, 5'-TCTTGC GACTCACGCTTGAC-3' and GADPH forward, 5'-AAA GATGTGCTTCGAGATGTGT-3' and reverse, 5'-CACTTT GTCAGTTACCAACGTCA-3'.

Western blot analysis. hBMVECs were lysed using RIPA lysis buffer (Beyotime Institute of Biotechnology). The protein concentration was calculated using a BCA assay and adjusted at

a final concentration of 0.5 mg/ml. The protein extracts (20 μg) were separated by 10% SDS-PAGE and subsequently blocked with 5% BSA at room temperature for 1 h. The expression of the target proteins was detected using the corresponding antibodies against ZO-1 (cat. no. ab276131; 1:1,000; Abcam), Occludin (cat. no. ab167161; 1:1,000; Abcam), Claudin-5 (cat. no. ab131259; 1:1,000; Abcam), VE-cadherin (1:1,000; cat. no. ab232880, Abcam), Bcl-2, Bax (cat. no. ab32503; 1:1,000; Abcam), Cleaved caspase-3 (cat. no. ab2302; 1:500; Abcam), cleaved poly-ADP ribose polymerase (PARP; cat. no. ab32064; 1:1,000; Abcam), EZH2 (cat. no. ab191080; 1:500; Abcam), GADPH (cat. no. ab9485; 1:1,000; Abcam) at 4˚C overnight, followed by the use of HRP-conjugated goat anti rabbit secondary antibody at room temperature for 2 h (cat. no. ab7090; 1:10,000; Abcam). Finally, the protein bands were visualized utilizing an ECL reagent (Thermo Fisher Scientific, Inc.). The quantitative analysis of protein levels was performed using ImageJ software 1.46r (National Institutes of Health).

RNA immunoprecipitation (RIP) assay. The potential interaction between HOTAIR and EZH2 was evaluated using a RIP (RNA Binding Protein Immunoprecipitation Assay) kit (cat. no. KT102-01; Guangzhou Saicheng Biological Technology Co., Ltd.) according to the manufacturer's protocols. hBMVECs were resuspended in RIP lysis buffer on ice for 5 min. The supernatant was collected following cell lysate preparation using centrifugation at 4˚C for 10 min. Part of the supernatant was used as the Input group. Antibodies against EZH2 (5 μg; cat. no. ab191250; Abcam) or IgG (5 μg; cat. no. ab6715; Abcam) were incubated with magnetic beads for 2 h at room temperature. Subsequently, this antibody-magnetic bead complex was incubated in the presence of the supernatant collected. The immunoprecipitated complexes were collected following centrifugation at 14,000 x g at 4˚C for 5 sec. The beads were re-suspended in Proteinase K for digestion at 55˚C for 10 min, and RNA were extracted using TRIzol method and analyzed using RT-qPCR.

Transfections. At 24 h prior to transfection, hBMVECs ($5x10^4$ cells/ml) were seeded into six-well plates. When the cells reached 70-90% confluence, hBMVECs were transfected with small interfering (si)RNAs (75 pmol) against HOTAIR (si-HOTAIR-1, 5'-CAGCCCAAUUUAAGAAUUATT-3'; si-HOTAIR-2, 5'-GGAGUACAGAGAGAAUAAUTT-3') and its negative control (5'-CUAUGAUACCCAAGUAAUATT-3'), EZH2 overexpressing plasmids (pEGFP-N1-EZH2; 2500 ng/well) or with the corresponding control (empty plasmids, NC) vectors (Shanghai GenePharma Co., Ltd.) using Lipofectamine® 3000, according to manufacturer's instructions (Thermo Fisher Scientific, Inc.). After 24 h, cells were used to perform further experiment.

Cell Counting Kit-8 (CCK-8) assay. hBMVECs ($3x10^4$ cells/well) were seeded into 96-well plates and after incubation at 37˚C for 24 h, 10 μl CCK-8 solution was added into each well (Thermo Fisher Scientific, Inc.). Following incubation for an additional 2 h at 37˚C, the absorbance at a wavelength of 450 nm was measured in each well using a microplate reader (Thermo Fisher Scientific, Inc.).

Lactate dehydrogenase (LDH) activity. hBMVECs ($3x10^4$ cells/well) were seeded into 96 well plate. The cell culture plates were centrifuged for 5 min at 37˚C at 400 x g. Subsequently, a total of 120 μl supernatant from each well was added into the corresponding well of a 96-well plate. The levels of LDH were measured using a LDH cytotoxicity assay kit (cat. no. C0017; Beyotime Institute of Biotechnology). Each well was supplemented with 60 μl detection solution followed by incubation at 37˚C for 30 min. The absorbance in each well was measured using a microplate reader (Thermo Fisher Scientific, Inc.) at a wavelength of 490 nm.

Endothelial monolayer cell permeability assay. hBMVECs from each treatment group were seeded into a 24-well Transwell chamber (pore size, 0.4 μm; Corning, Inc.) at a density of $1x10^5$ cells/well. The cells were then incubated in Procell Life Science & Technology Co., Ltd. medium for 8 h in a humidified atmosphere containing 5% CO_2 at 37˚C to form a confluent cell monolayer. The upper chamber was supplemented with FITC-albumin solved in Procell Life Science & Technology Co., Ltd. medium containing no serum (0.5 mg/ml, Sigma-Aldrich; Merck KGaA), whilst the bottom chamber with D-Hank's solution (Beijing Solarbio Science & Technology, Co., Ltd.). The cells were then incubated at 37˚C and 5% CO_2 for 45 min before samples were aspirated from both chambers. The optical density was detected at 488 nm using a fluorospectrophotometer. The membrane permeability coefficient of monolayer endothelial was calculated as described by a previous study (25).

TUNEL staining. hBMVECs ($1x10^6$ cells) were washed with PBS and fixed with 4% paraformaldehyde for 30 min at room temperature. Following incubation with PBS containing 0.3% Triton X-100 for 5 min, cells were rinsed with PBS and supplemented with a TUNEL solution (Beyotime Institute of Biotechnology) and incubated for 60 min at 37˚C. DAPI (0.1 ug/ml) was used to stain nuclei for 5 min at room temperature in the dark. After Antifade Mounting Medium (Beyotime Institute of Biotechnology) was added to the sections, four random fields were chosen and the apoptotic cells were observed under a fluorescence microscope (magnification, x200; Olympus Corporation).

Transwell assay. The invasive ability of hBMVECs was evaluated using Transwell assays (Costar; Corning Inc.). Matrigel (Costar; Corning Inc.) was first melted overnight at 4˚C and diluted in Procell Life Science & Technology Co., Ltd. medium with serum-free at a ratio of 1:8. Subsequently, the diluted Matrigel (40 μl/well) was coated onto the upper chamber of the Transwell chamber. The Transwell chamber was then placed in an incubator at 37˚C for 60 min for solidification. Subsequently, $1x10^4$ hBMVECs suspended in serum-free Procell Life Science & Technology Co., Ltd. medium were added into the upper chamber. A total of 600 μl Procell Life Science & Technology Co., Ltd. medium containing 10% FBS was added to the lower chamber. Following incubation for 24 h at 37˚C, the invasive cells were fixed with 4% paraformaldehyde for 20 min at room temperature followed by staining with 0.1% crystal violet for 15 min at room temperature. Five fields were randomly

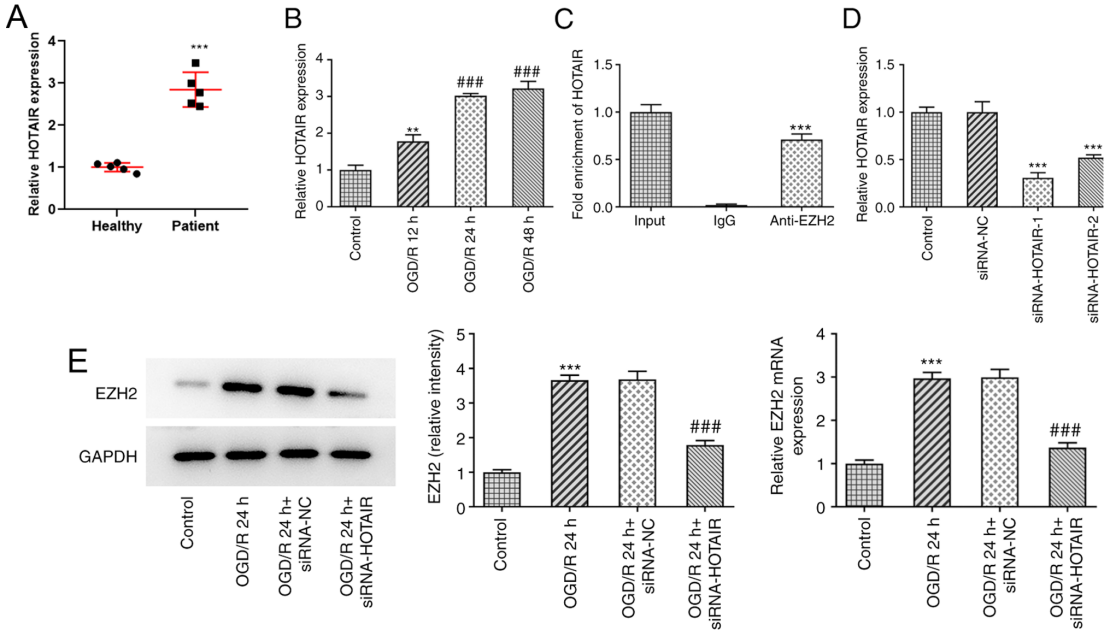

Figure 1. Ischemia/reperfusion conditions increases HOTAIR expression. (A) Reverse transcription-quantitative PCR analysis of HOTAIR expression in patients with HIE. ***P<0.001 vs. Healthy. (B) After hBMVECs were subjected to OGD/R, HOTAIR expression was measured using RT-qPCR. **P<0.01 vs. Control and ###P<0.001 vs. OGD/R 12 h. (C) RNA co-immunoprecipitation was performed to evaluate the potential interaction between HOTAIR and EZH2. ***P<0.001 vs. IgG. (D) The effects of siRNA-HOTAIR transfection on HOTAIR expression were measured using RT-qPCR. ***P<0.001 vs. siRNA-NC. (E) The expression of EZH2 was measured by western blotting after siRNA-HOTAIR transfection in hBMVECs treated with OGD/R. ***P<0.001 vs. Control. ###P<0.001 vs. OGD/R 24 h + siRNA-NC. HOTAIR, Hox transcript antisense intergenic RNA; EZH2, enhancer of zeste homolog 2; si, small interfering RNA; OGD/R, oxygen-glucose deprivation/reperfusion; NC, negative control; hBMVECs, human brain microvascular endothelial cells; RT-qPCR, reverse transcription-quantitative PCR.

selected and the invaded cells were observed under an inverted light microscope (magnification, x100; Olympus Corporation).

Tube formation assay. Matrigel was melted at 4˚C and subsequently used to coat 96-well plates at 37˚C (80 μl Matrigel/well; 10 mg/ml). Following incubation for 30 min, 200 μl of the cell suspension (Procell Life Science & Technology Co., Ltd. medium) was added into each well ($1x10^4$ cells/well). After 4 h at 37˚C, the formed tubes were observed under an inverted microscope (magnification, x40; Olympus Corporation). Four randomly selected fields were chosen and the tube quantities were calculated as the number of branch points in which at least 3 tubes joined.

Statistical analysis. All data were statistically analyzed using GraphPad Prism 7 software (GraphPad Software, Inc.). All experimental data are expressed as the mean ± SD. Each experiment was repeated at least three times. The differences among multiple groups were compared by one-way ANOVA followed by Tukey's post hoc test. P<0.05 was considered to indicate a statistically significant difference.

Results

HOTAIR expression is upregulated in the plasma of patients with neonatal HIE and in an vitro model of OGD/R injury. HOTAIR expression was found to be markedly upregulated in the plasma of patients with neonatal HIE compared with that in healthy neonates (Fig. 1A), suggesting a role for HOTAIR in HIE.

To assess the effects of IR on HOTAIR expression, hBMVECs were exposed to OGD/R before the expression levels of HOTAIR were determined by RT-qPCR (Fig. 1B). The results demonstrated that OGD/R exposure increased the expression level of HOTAIR in a time-dependent manner, compared with control group. It has been previously reported that HOTAIR can interact with EZH2 (26,27). Therefore, the potential interaction between HOTAIR and EZH2 was assessed by RIP assays. The results demonstrated that HOTAIR was markedly enriched in the samples immunoprecipitated using the EZH2 antibody, compared with the control IgG, according to results from the RT-qPCR assay (Fig. 1C). The transfection efficacy of siRNA-HOTAIR-1 or -2 was then evaluated using RT-qPCR. As shown in Fig. 1D, both siRNA-HOTAIR-1 and -2 significantly reduced HOTAIR expression compared with that in the siRNA-NC group. However, the effects of siRNA-HOTAIR-1 were superior compared with those mediated by siRNA-HOTAIR-2. To further investigate whether EZH2 could mediate the effects of HOTAIR on HIE, hBMVECs were transfected with si-HOTAIR before the expression levels of EZH2 were detected. RT-qPCR and western blot assays revealed that EZH2 expression was significantly upregulated in OGD/R-treated cells compared with that in control cells (Fig. 1E). However, these effects were significantly reversed following HOTAIR silencing.

EZH2 overexpression attenuates the effects of HOTAIR knockdown on cell viability and LDH release. To investigate if EZH2 overexpression can modulate the effects of HOTAIR silencing, an *in vitro* model of OGD/R injury was established

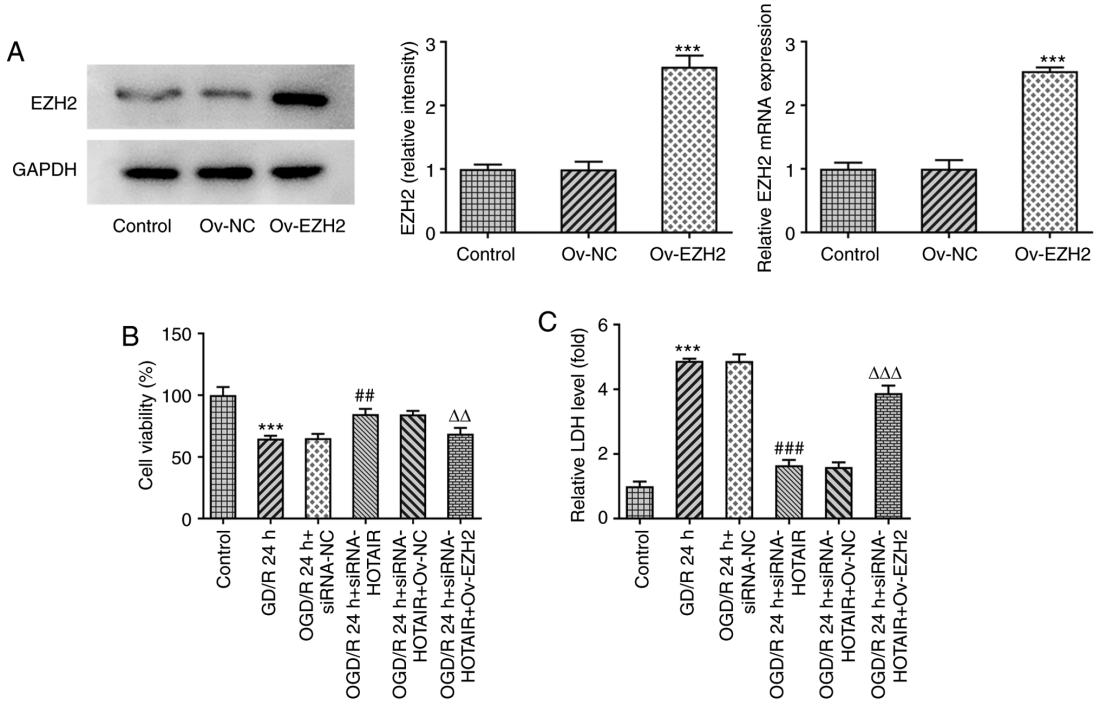

Figure 2. HOTAIR silencing alleviates human brain microvascular endothelial cells injury in an EZH2-dependent manner. (A) The expression of EZH2 after Ov-EZH2 transfection was measured by western blotting. ***P<0.001 vs. Ov-NC. (B) Analysis of cell viability using Cell Counting Kit-8 assay. ***P<0.001 vs. Control, ##P<0.01 vs. OGD/R 24 h + siRNA-NC, ΔΔP<0.01 vs. OGD/R 24 h + siRNA-HOTAIR + Ov-NC. (C) LDH release levels. ***P<0.001 vs. Control, ###P<0.001 vs. OGD/R 24 h + siRNA-NC, ΔΔΔP<0.001 vs. OGD/R 24 h + siRNA-HOTAIR + Ov-NC.. HOTAIR, Hox transcript antisense intergenic RNA; EZH2, enhancer of zeste homolog 2; si, small interfering RNA; OGD/R, oxygen-glucose deprivation/reperfusion; NC, negative control; Ov, overexpression; NC, negative control; LDH, lactate dehydrogenase.

to measure the changes in endothelial cell viability and LDH release following the transfection and subsequent OGD/R induction with an EZH2 overexpression plasmid. As shown in Fig. 2A, EZH2 was significantly overexpressed in cells transfected with EZH2 overexpression plasmids compared with that in cells transfected with the negative control plasmid. Although HOTAIR knockdown significantly enhanced cell viability whilst also significantly attenuating the release of LDH from OGD/R-treated hBMVECs, EZH2 overexpression significantly reversed both of the effects aforementioned (Fig. 2B and C). These findings suggest that EZH2 overexpression can regulate cell viability and LDH release from OGD/R-treated hBMVECs by interacting with HOTAIR.

HOTAIR silencing maintains the integrity of BBB via EZH2. BBB injury and aberrant changes in its permeability are considered to be processes that occur during cerebral IR injury and one of the main causes of mortality (28). To investigate whether EZH2 could mediate the effects of HOTAIR, an *in vitro* model of BBB was established to detect changes in the endothelial barrier integrity of OGD/R-induced hBMVECs following HOTAIR silencing and EZH2 overexpression. Subsequently, cell permeability and the expression levels of tight junction-proteins were measured by RT-qPCR and western blot analysis. The results demonstrated that HOTAIR silencing significantly reduced endothelial cell permeability compared with that in si-NC-transfected cells following OGD/R induction (Fig. 3A). In addition, HOTAIR silencing significantly increased the expression of zonula occludens-1 (ZO-1), occludin, claudin-5 and VE-cadherin in OGD/R-treated hBMVECs (Fig. 3B and C). However, all of the aforementioned effects were significantly reversed by EZH2 overexpression.

Since HOTAIR silencing appears to have improved the endothelial barrier integrity of OGD/R-induced hBMVECs, the effect of HOTAIR knockdown on hBMVEC apoptosis was then investigated. As shown in Fig. 4, HOTAIR knockdown significantly attenuated cell apoptosis compared with that in si-NC-transfected cells following OGD/R induction according to TUNEL assay. HOTAIR knockdown also significantly decreased the expression levels of the apoptosis-related proteins, Bax, cleaved caspase-3 and cleaved poly (adenosine diphosphate-ribose) polymerase whilst significantly increasing those of Bcl-2 (Fig. 5). All of these effects aforementioned were significantly reversed by EZH2 overexpression.

HOTAIR knockdown attenuates the migratory and angiogenic abilities of OGD/R-induced hBMVECs via EZH2. Since the regulatory effect of HOTAIR and EZH2 on OGD/R-induced hBMVEC layer integrity and apoptosis was uncovered, the present study next aimed to further investigate the role of HOTAIR in the migratory and tube formation capabilities of hBMVECs. It was found that transfection with si-HOTAIR significantly enhanced the migratory and tube formation abilities of hBMVECs compared with those in the si-NC group (Fig. 6A). However, these effects were significantly reversed following EZH2 overexpression (Fig. 6B). Overall, these results suggest that EZH2 can mediate the downstream physiological effects of HOTAIR on the migratory and tube formation abilities of hBMVECs.

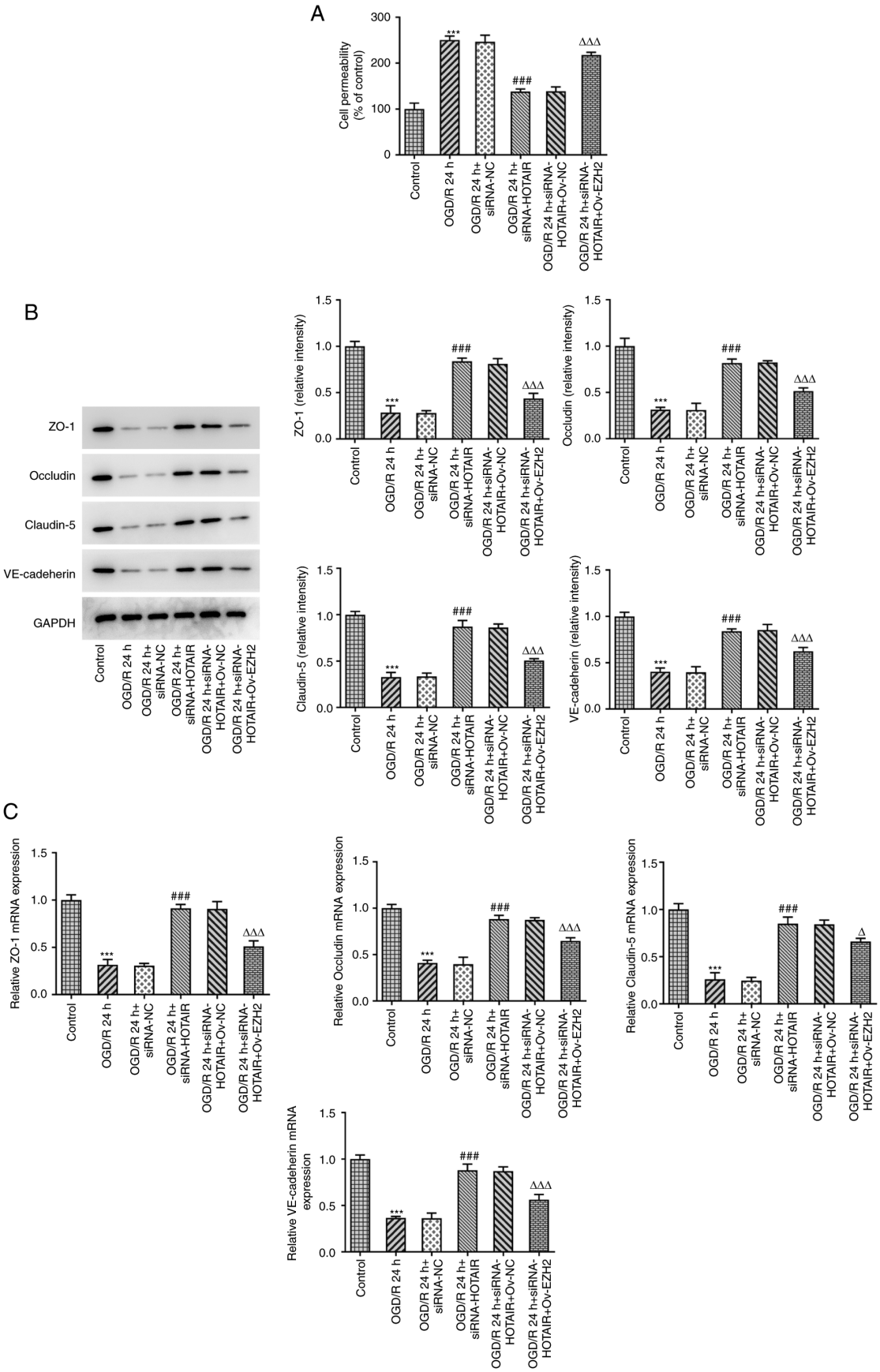

Figure 3. HOTAIR knockdown reduces the permeability of the hBMVEC layer and increases the expression of tight function proteins. (A) Analysis of HBMVECs permeability using Transwell assay. The expression of tight function proteins ZO-1, occludin, claudin-5 and VE cadherin were measured using (B) Western blotting and (C) reverse transcription-quantitative PCR. ***P<0.001 vs. Control, $^{###}$P<0.001 vs. OGD/R 24 h + siRNA-NC, ^{Δ}P<0.05 and ^{ΔΔΔ}P<0.001 vs. OGD/R 24 h + siRNA-HOTAIR + Ov-NC. HOTAIR, Hox transcript antisense intergenic RNA; EZH2, enhancer of zeste homolog 2; si, small interfering RNA; OGD/R, oxygen-glucose deprivation/reperfusion; NC, negative control; Ov, overexpression; NC, negative control; hBMVECs, human brain microvascular endothelial cells; ZO-1, zonula occludens-1; VE, vascular endothelial.

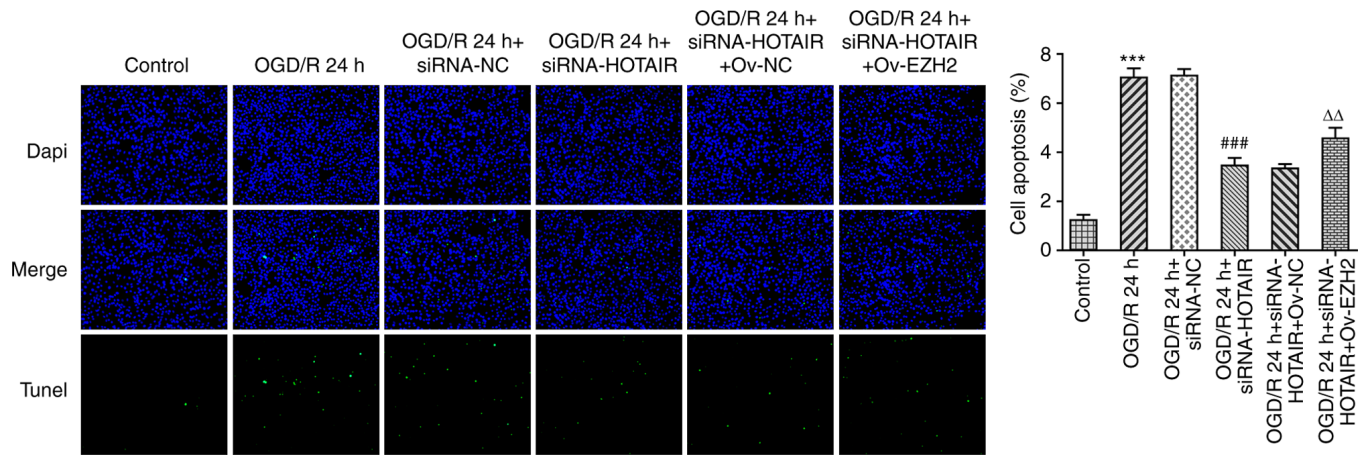

Figure 4. Effects of HOTAIR silencing and/or EZH2 overexpression on hBMVEC apoptosis. Evaluation of HBMVECs apoptosis using TUNEL assay. Magnification, x200. ***P<0.001 vs. Control, ###P<0.001 vs. OGD/R 24 h + siRNA-NC and ΔΔP<0.01 vs. OGD/R 24 h + siRNA-HOTAIR + Ov-NC. HOTAIR, Hox transcript antisense intergenic RNA; EZH2, enhancer of zeste homolog 2; si, small interfering RNA; OGD/R, oxygen-glucose deprivation/reperfusion; NC, negative control; Ov, overexpression; NC, negative control; hBMVECs, human brain microvascular endothelial cells.

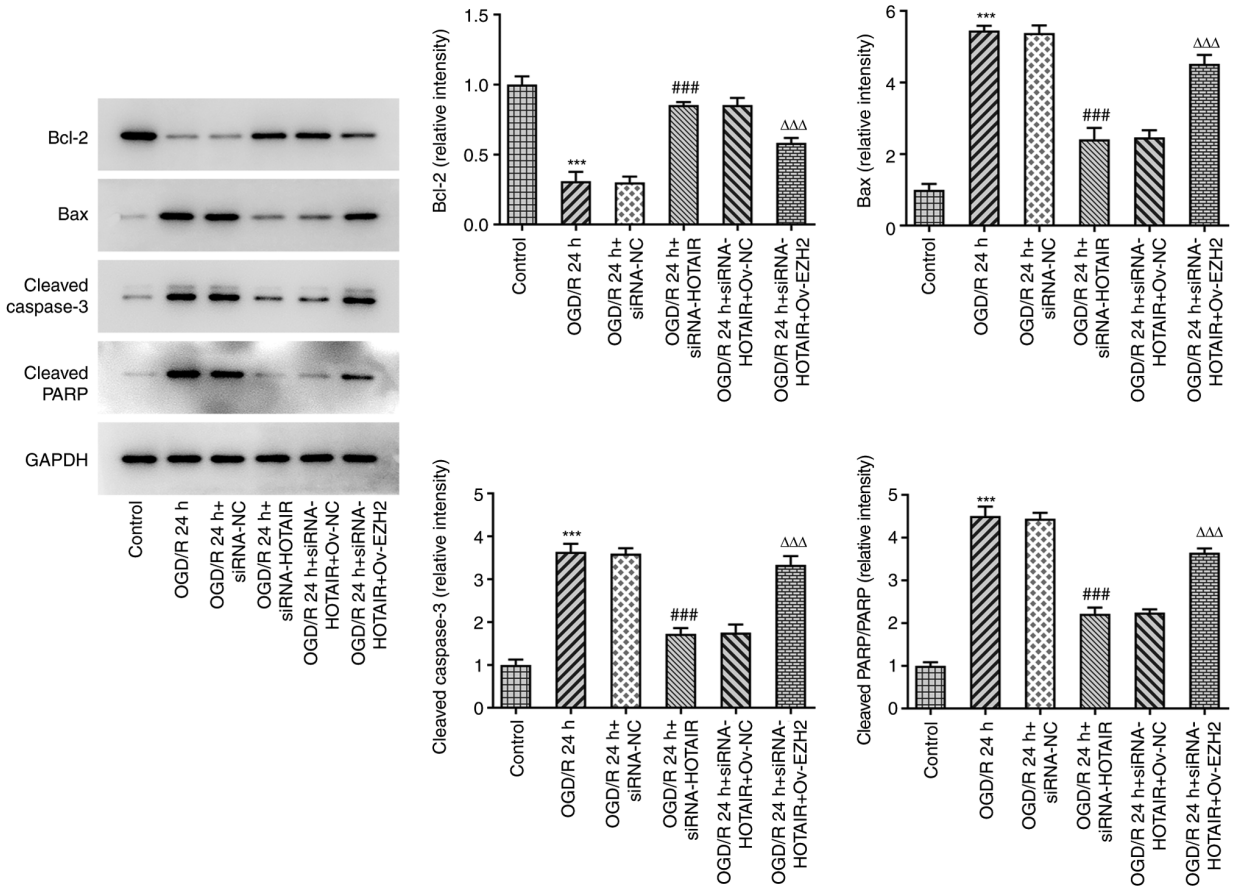

Figure 5. Effects of HOTAIR silencing and/or EZH2 overexpression on the expression of proteins associated with apoptosis in hBMVECs. Evaluation of HBMVECs apoptosis-related proteins Bcl-2, Bax, cleaved caspase-3 and cleaved PARP were measured by western blotting assay. ***P<0.001 vs. Control, ###P<0.001 vs. OGD/R 24 h + siRNA-NC and ΔΔΔP<0.001 vs. OGD/R 24 h + siRNA-HOTAIR + Ov-NC. HOTAIR, Hox transcript antisense intergenic RNA; EZH2, enhancer of zeste homolog 2; si, small interfering RNA; OGD/R, oxygen-glucose deprivation/reperfusion; NC, negative control; Ov, overexpression; NC, negative control; hBMVECs, human brain microvascular endothelial cells; PARP, poly-ADP ribose polymerase.

Discussion

Neonatal HIE is a type of cerebral hypoxic-ischemic injury that is caused by perinatal and is associated with poor prognosis (29). Among children with HIE, the mortality rate is typically 15-20% during the neonatal period in China (30). This relatively high mortality rate of HIE has been reported to be mainly due to delayed diagnosis and treatment of this

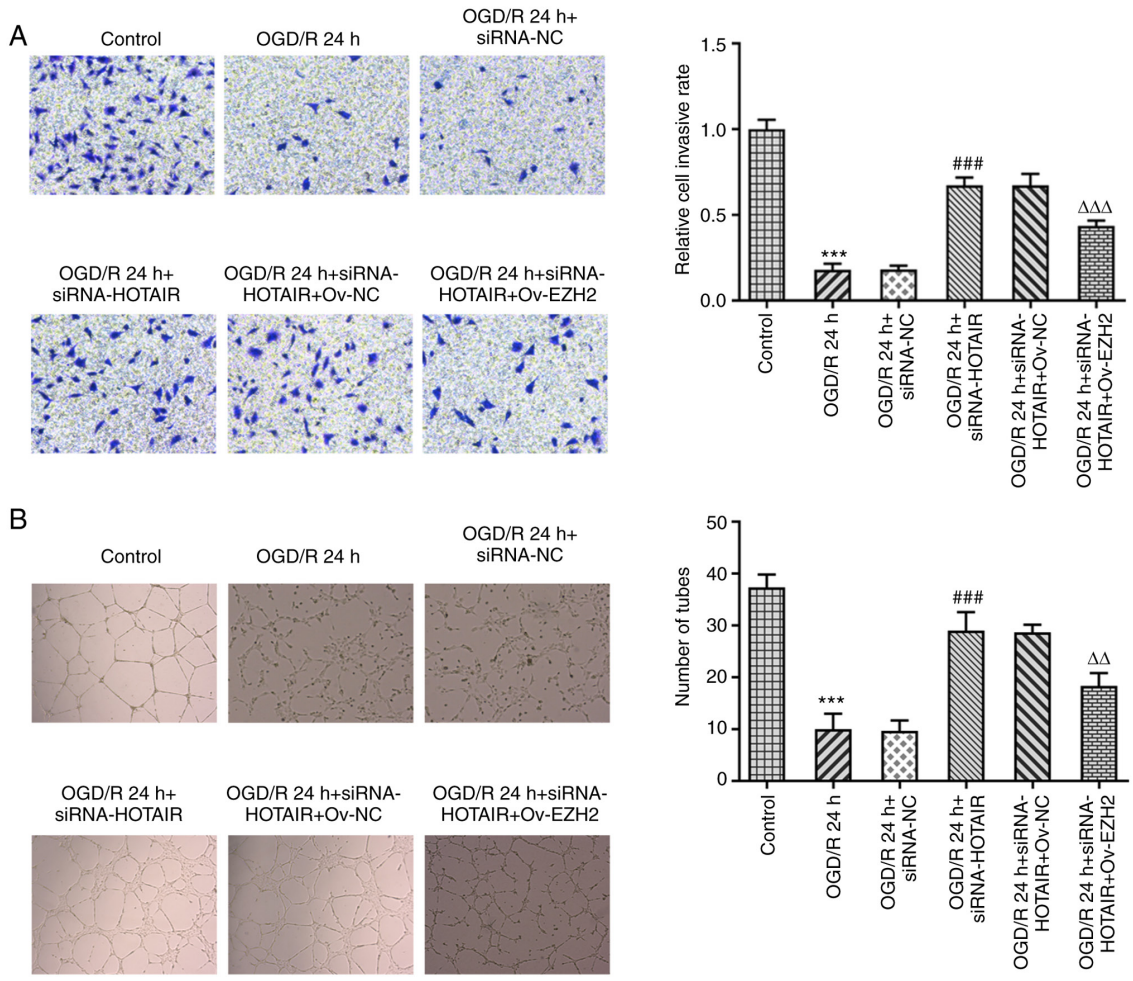

Figure 6. EZH2 overexpression reverses the increased cell migration and angiogenesis induced by HOTAIR silencing. (A) Analysis of hBMVEC invasion using a Transwell assay. Magnification, x100. (B) Measurement of tube formation capabilities of hBMVECs. Magnification, x40. ***P<0.001 vs. Control, $^{###}$P<0.001 vs. OGD/R 24 h + siRNA-NC, and ^{ΔΔ}P<0.01 and ^{ΔΔΔ}P<0.001 vs. OGD/R 24 h + siRNA-HOTAIR + Ov-NC. HOTAIR, Hox transcript antisense intergenic RNA; EZH2, enhancer of zeste homolog 2; si, small interfering RNA; OGD/R, oxygen-glucose deprivation/reperfusion; NC, negative control; Ov, overexpression; NC, negative control; hBMVECs, human brain microvascular endothelial cells.

condition (31). Therefore, early diagnosis and assessment of HIE severity and prognosis is of great clinical significance for improving the survival rate and quality of life of neonates. However, reperfusion is frequently accompanied by reperfusion injury (32). BMVECs normally maintain the structure of the BBB and express tight junction-related proteins, including VE-cadherin, ZO-1 and occludin (33,34). The present study revealed that HOTAIR was significantly upregulated in patients with neonatal HIE and an *in vitro* model of IR injury, which was consistent with those from previous studies (35-39), supporting a potential role of HOTAIR in IR injury.

Although there were statistical differences in HOTAIR expression between patients with neonatal HIE and healthy individuals, the relatively small sample size is a limitation of the present study. Results of a previous study demonstrated that HOTAIR interacts with EZH2 (40); thus, further experiments were performed to evaluate whether this interaction was also present in OGD/R-induced hBMVECs. The results showed that within hours following OGD/R, HOTAIR silencing could attenuate hBMVEC injury, as evidenced by the reduced hBMVEC permeability and apoptosis observed, in addition to the enhanced cell migration and angiogenesis. In addition, results from the RIP assays verified the interaction between HOTAIR and EZH2 in hBMVECs exposed to OGD/R. However, EZH2 overexpression reversed the effects of therapeutic effects of HOTAIR silencing on cell injury and tube formation ability of OGD/R-stimulated hBMVECs. By silencing HOTAIR in hBMVECs induced by OGD/R, the expression of EZH2 was reduced. Furthermore, hBMVECs exhibited higher EZH2 levels compared with control following OGD/R exposure. Therefore, there may possibly be a positive association between EZH2 and HOTAIR expression underlying the pathological process of patients with neonatal HIE, which warrants further study. HOTAIR has been documented to be an EZH2-binding lncRNA (40), where it regulates EZH2 expression and recruits EZH2 to MYC promoter sites (23). A previous report showed that lncRNA HERES regulates EZH2 protein levels through an interaction between the G-rich motif on the lncRNA and the N-terminal region of EZH2 (20). However, it remains unclear if there exists a direct site of interaction between HOTAIR and EZH2, which also require further study. Additionally, the effects

of EZH2 silencing on HOTAIR overexpression in OGD/R induced hBMVECs remains unknown, which is another limitation of the present study.

It has been previously reported that HOTAIR exerts a regulatory role in IR injury by regulating cell apoptosis and oxidative stress in the ischemic myocardium of rats (41). Notably, miR-130a-3p mediated the effects of HOTAIR on IR injury (41). To the best of our knowledge. the present study was the first to demonstrate that the HOTAIR/EZH2 axis may be involved in OGD/R-mediated endothelial dysfunction. ZO-1 was the first tight junction adhesion protein reported and is an important structural protein in the tight junction complex that is frequently used for evaluating BBB damage and function (42,43). A previous study demonstrated that the expression levels of ZO-1, occludin and claudin 5 mediated the tight junction, and were associated with cerebral IR injury in terms of BBB permeability (35). VE-cadherin is an adherens junction-associated protein that serves an important role in maintaining vascular integrity in vascular endothelial cells (44,45). The present study revealed that the HOTAIR/EZH2 axis could damage the structure of tight and adherens junctions by downregulating ZO-1, occludin, claudin 5 and VE-cadherin expression. However, a lack of *in vivo* data to validate this observation further is a limitation of the present study.

In conclusion, the present study revealed that the lncRNA HOTAIR may be involved in hBMVEC injury and apoptosis to mediate BBB damage through EZH2.

Acknowledgements

Not applicable.

Funding

The present study was approved by Science and Technology Innovation Bureau Foundation of Nanshan District Shenzhen (grant no. 2020118).

Availability of data and materials

The datasets used and/or analyzed during the current study are available from the corresponding author on reasonable request.

Authors' contributions

YPW, JYM, XDL, BBW and XGZ made substantial contributions to the conception and design of the study, performed the experiments and interpreted the data, and drafted and revised the manuscript for important intellectual content. YPW and XGZ confirm the authenticity of all the raw data. All authors read and approved the final manuscript.

Ethics approval and consent to participate

The present study was approved by the Ethics Committee of Huazhong University of Science and Technology Union Shenzhen Hospital (Shenzhen, China). Written informed consent for blood collection was obtained from the legal guardian of each child.

Patient consent for publication

Not applicable.

Competing interests

The authors declare that they have no competing interests.

References

1. Dumbuya JS, Chen L, Wu JY and Wang B: The role of G-CSF neuroprotective effects in neonatal hypoxic-ischemic encephalopathy (HIE): Current status. J Neuroinflammation 18: 55, 2021.
2. Ohshima M, Tsuji M, Taguchi A, Kasahara Y and Ikeda T: Cerebral blood flow during reperfusion predicts later brain damage in a mouse and a rat model of neonatal hypoxic-ischemic encephalopathy. Exp Neurol 233: 481-489, 2012.
3. Lv H, Wang Q, Wu S, Yang L, Ren P, Yang Y, Gao J and Li L: Neonatal hypoxic ischemic encephalopathy-related biomarkers in serum and cerebrospinal fluid. Clin Chim Acta 450: 282-297, 2015.
4. Hua C, Ju WN, Jin H, Sun X and Zhao G: Molecular chaperones and hypoxic-ischemic encephalopathy. Neural Regen Res 12: 153-160, 2017.
5. Dong MX, Hu QC, Shen P, Pan JX, Wei YD, Liu YY, Ren YF, Liang ZH, Wang HY, Zhao LB and Xie P: Recombinant tissue plasminogen activator induces neurological side effects independent on thrombolysis in mechanical animal models of focal cerebral infarction: A systematic review and meta-analysis. PLoS One 11: e0158848, 2016.
6. Arba F, Leigh R, Inzitari D, Warach SJ, Luby M and Lees KR; STIR/VISTA Imaging Collaboration: Blood-brain barrier leakage increases with small vessel disease in acute ischemic stroke. Neurology 89: 2143-2150, 2017.
7. Graves SI and Baker DJ: Implicating endothelial cell senescence to dysfunction in the ageing and diseased brain. Basic Clin Pharmacol Toxicol 127: 102-110, 2020.
8. Doll DN, Hu H, Sun J, Lewis SE, Simpkins JW and Ren X: Mitochondrial crisis in cerebrovascular endothelial cells opens the blood-brain barrier. Stroke 46: 1681-1689, 2015.
9. Tarafdar A and Pula G: The role of NADPH oxidases and oxidative stress in neurodegenerative disorders. Int J Mol Sci 19: 3824, 2018.
10. Liu C, Yang J, Zhang C, Liu M, Geng X, Ji X, Du H and Zhao H: Analysis of long non-coding RNA expression profiles following focal cerebral ischemia in mice. Neurosci Lett 665: 123-129, 2018.
11. Soudyab M, Iranpour M and Ghafouri-Fard S: The role of long non-coding RNAs in breast cancer. Arch Iran Med 19: 508-517, 2016.
12. Huang T, Zhao HY, Zhang XB, Gao XL, Peng WP, Zhou Y, Zhao WH and Yang HF: LncRNA ANRIL regulates cell proliferation and migration via sponging miR-339-5p and regulating FRS2 expression in atherosclerosis. Eur Rev Med Pharmacol Sci 24: 1956-1969, 2020.
13. Zhang W, Chen Y, Liu P, Chen J, Song L, Tang Y, Wang Y, Liu J, Hu FB and Hui R: Variants on chromosome 9p21.3 correlated with ANRIL expression contribute to stroke risk and recurrence in a large prospective stroke population. Stroke 43: 14-21, 2012.
14. Jiang B, Tang Y, Wang H, Chen C, Yu W, Sun H, Duan M, Lin X and Liang P: Down-regulation of long non-coding RNA HOTAIR promotes angiogenesis via regulating miR-126/SCEL pathways in burn wound healing. Cell Death Dis 11: 61, 2020.
15. Jin D, Wei W, Song C, Han P and Leng X: Knockdown EZH2 attenuates cerebral ischemia-reperfusion injury via regulating microRNA-30d-3p methylation and USP22. Brain Res Bull 169: 25-34, 2021.
16. Chen J, Zhang M, Zhang X, Fan L, Liu P, Yu L, Cao X, Qiu S and Xu Y: EZH2 inhibitor DZNep modulates microglial activation and protects against ischaemic brain injury after experimental stroke. Eur J Pharmacol 857: 172452, 2019.
17. Luo Y, Fang Y, Kang R, Lenahan C, Gamdzyk M, Zhang Z, Okada T, Tang J, Chen S and Zhang JH: Inhibition of EZH2 (enhancer of zeste homolog 2) attenuates neuroinflammation via H3k27me3/SOCS3/TRAF6/NF-κB (trimethylation of histone 3 lysine 27/suppressor of cytokine signaling 3/tumor necrosis factor receptor family 6/nuclear factor-κB) in a rat model of subarachnoid hemorrhage. Stroke 51: 3320-3331, 2020.

18. Yu YL, Chou RH, Shyu WC, Hsieh SC, Wu CS, Chiang SY, Chang WJ, Chen JN, Tseng YJ, Lin YH, *et al*: Smurf2-mediated degradation of EZH2 enhances neuron differentiation and improves functional recovery after ischaemic stroke. EMBO Mol Med 5: 531-547, 2013.
19. Xue H, Xu Y, Wang S, Wu ZY, Li XY, Zhang YH, Niu JY, Gao QS and Zhao P: Sevoflurane post-conditioning alleviates neonatal rat hypoxic-ischemic cerebral injury via Ezh2-regulated autophagy. Drug Des Devel Ther 13: 1691-1706, 2019.
20. Li Z, Hou P, Fan D, Dong M, Ma M, Li H, Yao R, Li Y, Wang G, Geng P, *et al*: The degradation of EZH2 mediated by lncRNA ANCR attenuated the invasion and metastasis of breast cancer. Cell Death Differ 24: 59-71, 2017.
21. Xue W, Wang F, Han P, Liu Y, Zhang B, Gu X, Wang Y, Li M, Zhao Y and Cui B: The oncogenic role of lncRNA FAM83C-AS1 in colorectal cancer development by epigenetically inhibits SEMA3F via stabilizing EZH2. Aging (Albany NY) 12: 20396-20412, 2020.
22. You BH, Yoon JH, Kang H, Lee EK, Lee SK and Nam JW: HERES, a lncRNA that regulates canonical and noncanonical Wnt signaling pathways via interaction with EZH2. Proc Natl Acad Sci USA 116: 24620-24629, 2019.
23. Papazian O: Neonatal hypoxic-ischemic encephalopathy. Medicina (B Aires) 78 (Suppl 2): 36-41, 2018 (In Spanish).
24. Livak KJ and SchmittgenTD: Analysis of relative gene expression data using real-time quantitative PCR and the 2(-Delta Delta C(T)) method. Methods 25: 402-408, 2001.
25. Ing NH, Berghman L, Abi-Ghanem D, Abbas K, Kaushik A, Riggs PK and Puschett JB: Marinobufagenin regulates permeability and gene expression of brain endothelial cells. Am J Physiol Regul Integr Comp Physiol 306: R918-R924, 2014.
26. Qian L, Fei Q, Zhang H, Qiu M, Zhang B, Wang Q, Yu Y, Guo C, Ren Y, Mei M, *et al*: lncRNA HOTAIR promotes DNA repair and radioresistance of breast cancer via EZH2. DNA Cell Biol: Nov 2, 2020 (Epub ahead of print).
27. Zhao YH, Liu YL, Fei KL and Li P: Long non-coding RNA HOTAIR modulates the progression of preeclampsia through inhibiting miR-106 in an EZH2-dependent manner. Life Sci 253: 117668, 2020.
28. Bernardo-Castro S, Sousa JA, Brás A, Cecília C, Rodrigues B, Almendra L, Machado C, Santo G, Silva F, Ferreira L, *et al*: Pathophysiology of blood-brain barrier permeability throughout the different stages of ischemic stroke and its implication on hemorrhagic transformation and recovery. Front Neurol 11: 594672, 2020.
29. Nakamura S, Koyano K, Jinnai W, Hamano S, Yasuda S, Konishi Y, Kuboi T, Kanenishi K, Nishida T and Kusaka T: Simultaneous measurement of cerebral hemoglobin oxygen saturation and blood volume in asphyxiated neonates by near-infrared time-resolved spectroscopy. Brain Dev 37: 925-932, 2015.
30. Park WS, Sung SI, Ahn SY, Yoo HS, Sung DK, Im GH, Choi SJ and Chang YS: Hypothermia augments neuroprotective activity of mesenchymal stem cells for neonatal hypoxic-ischemic encephalopathy. PLoS One 10: e0120893, 2015.
31. Khan RH, Islam MS, Haque SA, Hossain MA, Islam MN, Khaleque MA, Chowdhury B and Chowdhury MA: Correlation between grades of intraventricular hemorrhage and severity of hypoxic ischemic encephalopathy in perinatal asphyxia. Mymensingh Med J 23: 7-12, 2014.
32. Catanese L, Tarsia J and Fisher M: Acute ischemic stroke therapy overview. Circ Res 120: 541-558, 2017.
33. Méresse S, Dehouck MP, Delorme P, Bensaïd M, Tauber JP, Delbart C, Fruchart JC and Cecchelli R: Bovine brain endothelial cells express tight junctions and monoamine oxidase activity in long-term culture. J Neurochem 53: 1363-1371, 1989.
34. Uwamori H, Ono Y, Yamashita T, Arai K and Sudo R: Comparison of organ-specific endothelial cells in terms of microvascular formation and endothelial barrier functions. Microvasc Res 122: 60-70, 2019.
35. Liu Z, Liu Y, Zhu Y and Gong J: HOTAIR/miRNA-1/Cx43: A potential mechanism for treating myocardial ischemia-reperfusion injury. Int J Cardiol 308: 11, 2020.
36. Ma NH, Zhang MH, Yang JX, Sun ZJ, Yuan F and Qiu XL: Long noncoding RNA HOTAIR sponging miR-211 regulates cerebral ischemia-reperfusion injury. J Biol Regul Homeost Agents 34: 2209-2214, 2020.
37. Meng K, Jiao J, Zhu RR, Wang BY, Mao XB, Zhong YC, Zhu ZF, Yu KW, Ding Y, Xu WB, *et al*: The long noncoding RNA hotair regulates oxidative stress and cardiac myocyte apoptosis during ischemia-reperfusion injury. Oxid Med Cell Longev 2020: 1645249, 2020.
38. Sun Y and Hu ZQ: LncRNA HOTAIR aggravates myocardial ischemia-reperfusion injury by sponging microRNA-126 to upregulate SRSF1. Eur Rev Med Pharmacol Sci 24: 9046-9054, 2020.
39. Tang B, Bao N, He G and Wang J: Long noncoding RNA HOTAIR regulates autophagy via the miR-20b-5p/ATG7 axis in hepatic ischemia/reperfusion injury. Gene 686: 56-62, 2019.
40. Wang Y, Xie Y, Li L, He Y, Zheng D, Yu P, Yu L, Tang L, Wang Y and Wang Z: EZH2 RIP-seq identifies tissue-specific long non-coding RNAs. Curr Gene Ther 18: 275-285, 2018.
41. Fang J, Zheng W, Hu P and Wu J: Investigating the effect of lncRNA HOTAIR on apoptosis induced by myocardial ischemia-reperfusion injury. Mol Med Rep 23: 169, 2021.
42. Jiao H, Wang Z, Liu Y, Wang P and Xue Y: Specific role of tight junction proteins claudin-5, occludin, and ZO-1 of the blood-brain barrier in a focal cerebral ischemic insult. J Mol Neurosci 44: 130-139, 2011.
43. Reinhold AK and Rittner HL: Barrier function in the peripheral and central nervous system-a review. Pflugers Arch 469: 123-134, 2017.
44. Lampugnani MG, Dejana E and Giampietro C: Vascular endothelial (VE)-cadherin, endothelial adherens junctions, and vascular disease. Cold Spring Harb Perspect Biol 10: a029322, 2018.
45. Giannotta M, Trani M and Dejana E: VE-cadherin and endothelial adherens junctions: Active guardians of vascular integrity. Dev Cell 26: 441-454, 2013.